

**BASIC STUDY ON THE APPLICATION OF
ELECTRON ATTACHMENT REACTION TO THE
TREATMENT OF CREMATORY EMISSION GAS***
การศึกษาพื้นฐานเกี่ยวกับการประยุกต์ปฏิกิริยาเติมอิเล็กตรอน
กับการบำบัดก๊าซทิ้งจากเมรุเผาศพ

Wiwut Tanthapanichakoon
วิวัฒน์ ตันทะพานิชกุล

Kittisak Larpsuriyakul
กิตติศักดิ์ ลาภสุริยกุล

Paisarn Khongprasarnkal
ไพศาล คงประสานกาล

Tawatchai Charinpanitkul
ทวัชชัย ชรินพานิชกุล

Department of Chemical Engineering, Faculty of Engineering, Chulalongkorn University
ภาควิชาวิศวกรรมเคมี คณะวิศวกรรมศาสตร์ จุฬาลงกรณ์มหาวิทยาลัย

Hajime Tamon
ฮายิเมะ ทะมอน

Morio Okazaki
โมริโอะ โอคาซากิ

Department of Chemical Engineering, Faculty of Engineering, Kyoto University
ภาควิชาวิศวกรรมเคมี คณะวิศวกรรมศาสตร์ มหาวิทยาลัยเกียวโต

Noriaki Sano
โนริอากิ ซาโน

Department of Chemical Engineering, Faculty of Engineering
Himeji Institute of Technology
ภาควิชาวิศวกรรมเคมี คณะวิศวกรรมศาสตร์ สถาบันเทคโนโลยีฮิเมจิ

(ได้รับเมื่อ พฤศจิกายน 2540)

* ได้รับทุนอุดหนุนการวิจัยจากสำนักงานคณะกรรมการวิจัยแห่งชาติ ประจำปี 2540

ABSTRACT

Electron attachment reaction occurs when low-energy electrons generated in a corona-discharge reactor are captured by electronegative impurities, producing negative ions. The ions migrate in the electric field to the anode (reactor wall) and are removed at the wall. Basic study on the application of electron attachment to the treatment of gaseous pollutants including those present in crematory emission gases were carried out experimentally. Several important effects, namely, discharge current, inlet gas concentration, space velocity and coexisting O_2 or H_2O vapor on the removal efficiency have been investigated. The experimental results reveal that generally the higher the discharge current, the higher the removal efficiency, whereas the space velocity and inlet gas concentration yield the opposite results. It is found that the presence of O_2 or H_2O vapor may either enhance or retard the removal efficiency.

In addition, as a guideline for scaling up, the effects of the reactor structure, namely, the cathode diameter, the anode (reactor) shape and the number of cathodes on the removal efficiency with respect to three dilute gaseous pollutants, methyl iodide, chlorofluorocarbon and acetaldehyde, were investigated experimentally. The results reveal that the thicker the cathode diameter tested, the higher the removal efficiency. In contrast, the smaller the reactor diameter among three equivolume reactors, the higher the removal efficiency. As for the number of cathodes in a single reactor vessel, the single-cathode reactor exhibits higher removal efficiency than the 5-cathode one.

บทคัดย่อ

ปฏิกิริยาเติมอิเล็กตรอนเกิดขึ้นเมื่ออิเล็กตรอนพลังงานต่ำที่ผลิตในเครื่องปฏิกรณ์แบบปล่อยโคโรนาถูกโมเลกุลของก๊าซไม่บริสุทธิ์ชนิดอิเล็กโตรเนกาตีฟจับไว้ เป็นผลให้เกิดไอออนประจุลบขึ้น ไอออนประจุลบที่เกิดขึ้นนี้จะเคลื่อนที่ในสนามไฟฟ้าไปยังขั้วอะโนด (ผนังของเครื่องปฏิกรณ์) และถูกกำจัดออกที่ผนังนั้น ผู้วิจัยได้ทำการศึกษาเบื้องต้นเกี่ยวกับการประยุกต์ใช้การเติมอิเล็กตรอนกับการบำบัดก๊าซมลพิษ รวมทั้งองค์ประกอบของก๊าซที่เกิดจากการเผาปนพิษโดยการทดลอง ซึ่งการวิจัยนี้ครอบคลุมถึงผลกระทบที่สำคัญหลายอย่าง ได้แก่ กระแสปล่อยออก ความเข้มข้นของก๊าซขาเข้า อัตราการไหลของก๊าซ และปริมาณออกซิเจนหรือไอน้ำ ที่มีต่อประสิทธิภาพการกำจัด ผลการทดลองแสดงให้เห็นว่า โดยทั่วไปแล้ว หากกระแสปล่อยออกยิ่งสูง ประสิทธิภาพการกำจัดก็จะยิ่งสูงขึ้น ในขณะที่อัตราการไหลของก๊าซและความ

เข้มข้นของก๊าซเข้ากลับให้ผลตรงกันข้าม อนึ่ง ปริมาณออกซิเจนหรือไอน้ำอาจช่วยเพิ่มหรือลดประสิทธิภาพการกำจัดได้

นอกจากนี้ ยังได้ทำการทดลองเพื่อกำหนดแนวทางในการขยายขนาดของเครื่องปฏิกรณ์ ผลกระทบของโครงสร้างของเครื่องปฏิกรณ์ ได้แก่ เส้นผ่านศูนย์กลางของกะโหลก รูปทรงอะโนด (เครื่องปฏิกรณ์) และจำนวนของกะโหลก ที่มีต่อประสิทธิภาพการกำจัดก๊าซมลพิษความเข้มข้นต่ำ 3 ชนิดคือ อะเซทัลดีไฮด์ (CH_3CHO), เมทิลไอโอไดด์ (CH_3I) และคลอโรฟลูออโรคาร์บอน ($\text{C}_2\text{Cl}_3\text{F}_3$) ผลการทดลองแสดงให้เห็นว่าถ้าขนาดเส้นผ่านศูนย์กลางของกะโหลกที่ใช้ทดสอบยิ่งโตขึ้น ประสิทธิภาพการกำจัดก็จะยิ่งสูงขึ้น ตรงกันข้าม เมื่อเปรียบเทียบระหว่างเครื่องปฏิกรณ์ 3 เครื่องที่มีปริมาตรเท่ากัน พบว่าถ้าขนาดเส้นผ่านศูนย์กลางของเครื่องปฏิกรณ์ยิ่งเรียว ประสิทธิภาพการกำจัดก็จะยิ่งสูงขึ้น อนึ่ง เมื่อเปรียบเทียบผลของจำนวนกะโหลกในเครื่องปฏิกรณ์เครื่องเดียวกัน พบว่าเครื่องปฏิกรณ์ที่มีกะโหลกเดียวให้ประสิทธิภาพการกำจัดสูงกว่าเครื่องปฏิกรณ์ที่มี 5 กะโหลก

INTRODUCTION

Crematory emission gas

Like most countries Thailand has been facing various environmental problems due to the growth of human activities. For example, a sizable number of city vehicles and industrial plants releasing an unacceptable level of various gaseous pollutants as well as particulate matter significantly contribute to global impacts such as the greenhouse effect, acid rain, urban smog, and depletion of ozone layer in the stratosphere. It has been found that although the concentration levels of the gaseous pollutants are very low in the ppm or ppb orders, they not only lead to environmental deterioration but also cause public nuisances and, in many cases, may be detrimental to public health.

Recently, a latent source of public nuisance has become prominent. It is the crematoria of nearly 20,000 temples in Thailand, particularly the approximately 300 temples in the Bangkok Metropolitan Area. Besides particulates, malodorous gaseous components are emitted during cremation, causing frequent complaints from local communities. This is because emission from the furnace of the crematorium is directly released from the stack to the atmosphere without any treatment. It is reported that nearly all of the approximately 20,000 temples in Thailand lack appropriate emission control systems, including most of the nearly 300 temples in Bangkok having frequent crematory activities. A few rich temples have installed cremating furnaces with the

after-burning systems, which cost around 3~5 million baht per system. However, shortage of funds has impeded even the upgrading of the existing furnaces. Most temples nationwide and even some well-known ones in Bangkok still use firewood as the main fuel. Thus the chances of them installing the imported after-burning systems are slim, if not nil, unless some novel and economical control system can be developed to remove the dilute obnoxious gaseous components in crematory emission with high efficiency. The removal of particulates is easier but should also be achieved by the same system.

Though the problem is much less severe, similar complaints about crematory emission are heard in several countries, including Japan, the United Kingdom and Germany. In order to meet the emission control standards, a typical modern Japanese crematorium generally installs an after-burner furnace to decompose the malodorous organic gaseous components at high temperature. Next fresh air is drawn to cool down and further dilute the residual gaseous components by one or two orders of magnitude before sending the cooled-down gas through a dust collector^{7,8,9}

Nishida^{8,9} reports that exhaust gas from one gas-fired crematory in Japan consists of the following average gaseous composition after 100-fold dilution with fresh air.

High-concentration components:

N ₂	78%
O ₂	20~21%

Low-concentration components:

CO ₂	0.01~0.02%
H ₂ O	0.22%
NO _x	80 ppm (max)
SO _x	5.8 ppm (max)
Acetic acid (CH ₃ COOH)	24 ppm
Hydrocarbons	230 ppm (as propane)

Very low-concentration malodorous components:

Acetaldehyde (CH_3CHO)	0.04 ppm
Styrene ($\text{C}_6\text{H}_5\text{CH} = \text{CH}_2$)	0.01 ppm
Hydrogen sulfide (H_2S)	0.01 ppm
Methyl mercaptan (CH_3SH)	0.001 ppm
Dimethyl sulfide [$(\text{CH}_3)_2\text{S}$]	0.0005 ppm
Ammonia (NH_3)	0.37 ppm (max)
Trimethyl amine [$(\text{CH}_3)_3\text{N}$]	0.023 ppm (max)

It can be seen that, besides NO_x and SO_x , various kinds of dilute gas components are present as malodorous gases. It should be noted that the above concentrations of such malodorous gases have been diluted 100 times with ambient air. Hence, the concentrations are nearly 100 times higher before dilution.

Because of greater public awareness of nuisances and health risks associated with crematory emission, the Parliamentary Committee on Science and Technology, House of National Representatives, is much interested in some appropriate technology to solve the problem of the malodorous gases. This has motivated the authors to jointly carry out a basic study on the application of electron attachment reaction to the treatment of crematory emission gas.

Electron attachment reaction

The novel concept of gas purification by low-energy electron attachment was first proposed by Tamon et al.¹⁶ When low-energy electrons collide with gas molecules, some of them are captured by the molecules and negative ions are formed. This phenomenon is called "electron attachment"⁵ and it depends on the electron energy, the structure of the gas molecule, and its electron affinity. There is a huge difference in the attachment probability among different types of gas molecules, and this leads to high selectivity in the production of negative ions^{1,5,6}. Hence electronegative impurities of extremely low concentration can selectively become negative ions by electron attachment and they can effectively be separated from the neutral gas in an electric field.

Tamon et al.¹⁶ constructed two kinds of separation devices using either photocathode or glow discharge as electron source. They reported high efficiency for the removal from nitrogen of SF_6 of very low concentrations. Recently Tamon et al.¹⁷ used two types of corona-discharge reactors to remove sulfur compounds, iodine and oxygen from nitrogen. They also discussed the purification mechanism and presented simulation models for predicting the removal efficiency. Subsequently, Tamon et al.¹⁸ investigated the influence of coexisting oxygen and/or water vapor on the removal of several sulfur compounds. As a continuation, Sano et al.¹² used a new type of corona-discharge reactor, the wetted-wall reactor, and the conventional deposition-type reactor to remove iodine and methyl iodide from nitrogen.

Sano¹³ and Sano et al.^{14,15} have reported the production of various chemical species of negative ions during the removal of either CH_3I , $\text{C}_2\text{Cl}_3\text{F}_3$ or CH_3CHO from air or N_2 . For example, dissociative electron attachment of CH_3CHO may produce O^- , C_2O^- , HC_2O^- , CH_3CO^- , or CH_3^- . Similarly, I^- may be produced from CH_3I ; whereas Cl^- and F^- from $\text{C}_2\text{Cl}_3\text{F}_3$. In the removal of CH_3I from air and $\text{C}_2\text{Cl}_3\text{F}_3$ from N_2 , dark brown particles are formed on the reactor anode. On the other hand, in the removal of CH_3CHO from air, a brown coating is formed.

Gas purification via electron attachment mechanism relies on an entirely different working principle from those of the conventional gas separation methods, such as 1) gas absorption, 2) adsorption, 3) membrane separation, 4) distillation, 5) cryogenic separation. The new method possesses the distinction that it is capable of removing a variety of gaseous pollutants, including toxic gases, particularly at extremely low concentration levels (ppm or ppb orders). Whereas the conventional methods either have relatively low efficiency or are energy intensive at such low levels.

Since most malodorous components in the crematory emission are highly electronegative gaseous components, electron attachment seems to be one most effective way to remove them in an electric field. The present work aims at a basic study on the application of electron attachment reaction to the treatment of crematory emission. The first part of what follows is the various effects on the individual removal efficiency of the key components found in crematory emission by Nishida. The second part aims to obtain a guideline on how to scale up the electron attachment reactor. As a first step, the effect of the reactor structure on removal efficiency must be

understood. Any structural change is expected to affect simultaneously several important factors such as the discharge current, electron energy, electric field strength, migratory distance, and residence time in the reactor. The second part investigates the effects of the reactor structure, namely the cathode diameter, the anode (reactor) dimension and the number of cathodes on the resulting removal efficiency with respect to three dilute gaseous pollutants.

With further advancement of the technology and the use of multi-stage reactor, it is reasonable to aim at the simultaneous removal of both gaseous pollutants and fine particles since the basic principle of corona discharge and subsequent deposition on the anode is similar to that of an Electrostatic Precipitator (ESP)^{4,10,11,21}. This is however beyond the scope of this work.

Principle of gas purification

Figure 1 illustrates the principle of gas purification by removing an impurity, AB, from an inert gas in a cylindrical corona-discharge reactor¹⁷. The corona discharge method employed here is an efficient method to supply a sufficient number of low-energy electrons to the gas stream. A wire stretched along the axis of the reactor acts as cathode and the outer cylinder acts as grounded anode. High DC voltage applied to the cathode induces corona discharge in the reactor. Electrons generated at the cathode drift to the anode along the electric field. During their drift, a portion of them collides with gas molecules. Negative ions, A^- , are thus selectively produced by electron attachment and they likewise drift to the anode as the electrons do. If the number of electrons generated in the reactor is sufficient to collide successfully with all gaseous impurities and if all negative ions A^- produced completely deposit at the anode surface, complete removal is achieved.

Besides the above-mentioned removal mechanism associated with electron attachment reaction in the corona-discharge reactor, it is believed that other removal mechanisms may simultaneously affect the removal efficiency. When negative ions are produced in the reactor, they may possibly interact with other gas molecules via their electrostatic forces and negative-ion clusters may be formed. Each cluster then contains more than one of the gas molecules targeted for removal. When such clusters drift to the anode and deposit there, the removal efficiency is enhanced by the formation of negative-ion clusters.

Another possible mechanism contributing to the removal efficiency is the so-called radical reaction. When dissociative electron attachment also takes place in the reactor, not only negative ions but also reactive radicals are produced. In particular, radicals may readily be produced in the immediate vicinity of the cathode surface since high electric field strength exists there. It is logical to assume that removal efficiency would be affected by radical reaction.

The reaction of gas molecules with O_3 is frequently mentioned. Ozone reaction can take place when oxygen coexists in the gas stream. High energy electrons close to the cathode collide with O_2 molecules to dissociatively produce O radicals. O radicals can next react with O_2 molecules to produce O_3 , which is reactive with various kinds of gases. Hence, ozone reaction is expected to contribute to the destruction of a number of gaseous impurities in the gas stream, thus improving the removal efficiency.

PART I. INVESTIGATION ON INDIVIDUAL REMOVAL EFFICIENCY

What follows is a summary of the experimental results of individual removal for a variety of gases, including several components found in crematory emission. More specifically, the influences of several important factors, namely, discharge current, applied voltage, gas flow rate, inlet gas concentration, and some coexisting gases (e.g., oxygen and water vapor) on the removal efficiency of the individual targeted gases are examined experimentally. Note that some of the removal data have already been published elsewhere.^{2,3,12,14,15,16,17,18,19,20}

MATERIALS AND METHODS

Figure 2 shows a schematic diagram of the gaseous pollutant remover. A gas sample was mixed with N_2 , N_2-O_2 or N_2-H_2O in a gas mixing device and was then fed to the corona-discharge reactor. The coexisting oxygen or water vapor was introduced in order to examine its influence on the removal efficiency of each gas sample. Sulfur hexafluoride (SF_6), dimethyl sulfide $[(CH_3)_2S]$, carbonyl sulfide (COS), hydrogen sulfide (H_2S), methyl mercaptan (CH_3SH), carbon disulfide (CS_2), sulfur dioxide (SO_2), methyl iodide (CH_3I), acetaldehyde (CH_3CHO), chlorofluorocarbon ($C_2Cl_3F_3$), and trimethyl amine $(CH_3)_3N$ were investigated. The reactor consists of a 38-

mm-ID, 280-mm-long cylindrical anode (brass pipe) and a 0.3-mm-diameter wire cathode. A gas absorber was used to trap the residual impurities and possible by-products at the outlet of the reactor. The flow rate of the gas mixture was measured by a soap film flow meter.

The inlet concentrations of the gas samples were adjusted by mixing lab-grade gases with N_2 . The concentrations of individual sulfur or organic compounds (gas samples) at both the inlet and outlet of the reactor were determined by a gas chromatograph with a flame photometric detector (FPD) or with a flame ionization detector (FID), respectively. The inlet concentration of water vapor was controlled by bubbling the inert gas (N_2) in distilled water in a temperature-controlled bath. The concentration of water vapor was analyzed by a dew point hygrometer. The inlet concentrations of the gas samples, oxygen and water vapor ranged between 0.176~400 ppm, 0~49%, 300~13,000 ppm, respectively.

The removal efficiency, ψ , is defined by the following equation.

$$\psi = (C_{in} - C_{out}) / C_{in} \quad (1)$$

where C_{in} and C_{out} are the inlet and outlet concentrations of the pollutant in the gas sample.

In some cases, Eq. (1) may not be suitable if not only the gaseous pollutant but also reaction by-products are to be considered, for example, removal of sulfur compounds. In such cases, removal efficiency is defined as follows.

$$\psi^s = 1 - (C_{out} + kC_{sub}) / C_{in} \quad (2)$$

where C_{sub} is the total concentration of reaction by-products in the outlet gas. k is a stoichiometric number for sulfur. For example, when the by-products appear, k is $1/2$ for CS_2 removal, or 1 for other removals if, from the stoichiometric relation, one molecule of the reaction by-products contains one sulfur atom.

RESULTS AND DISCUSSION

The reactor pressure is atmospheric throughout all the experiments referred to in this paper. Figures 3 and 4, respectively, show the measured (experimental) and

the correlated (calculated) removal efficiency of SF_6 from N_2 as a function of the discharge current I and gas space velocity SV , corresponding to the specified inlet concentrations of SF_6 . In Figure 3, SV (the ratio of the gas flow rate to the reactor volume) is fixed at 18.9 h^{-1} . Obviously, the higher the discharge current I , the higher the removal efficiency ψ . This is because the probability of electron attachment increases with the increased number of free electrons available for collision with SF_6 molecules.

The correlated values of ψ in Figures 3 and 4 were obtained by Tamon et al.¹⁷ using the relevant kinetics and transport phenomena model. Though the measured and correlated values agree reasonably well, their model is applicable to the simple case (like SF_6) in which no clusters of negative ions are formed by electron attachment.

Tables 1-4 show, respectively, the effects of inlet gas concentration (C_{in}), space velocity (SV), coexisting oxygen (C_{O_2}), and coexisting water vapor ($C_{\text{H}_2\text{O}}$) on the experimental removal efficiency (ψ) and the type of reaction by-products detected. Table 5 shows the simultaneous effects of $C_{\text{H}_2\text{O}}$ and C_{O_2} on ψ and by-product type. In each table the ranges of I , SV , C_{in} , C_{O_2} , $C_{\text{H}_2\text{O}}$ indicate the ranges of the values used in the experiments. In the column on "removal efficiency", the "incr." or "decr." under the "change of ψ " with respect to " I ", " C_{in} " or " SV " means ψ was found to increase or decrease as the mentioned variable (I , C_{in} , or SV) increased. For example, the first row of Table 1 indicates that in the case of SF_6 , experiments were carried out at several SF_6 inlet concentrations (C_{in}), that at each C_{in} , ψ increased as I increased, and that at the same I , ψ decreased as C_{in} increased. ψ_{max} is the maximum value observed among all of these experiments. In fact, Tables 1-5 are unanimous that ψ increases as I increases.

Furthermore, Figure 3 shows that ψ increases as the inlet concentration, C_{in} , decreases. For example, when C_{in} is either 1 ppm or 176 ppb, about 99% of SF_6 is removed in the reactor. In short, if sufficient electrons compared with the electronegative gas molecules are supplied to the reactor, the removal efficiency improves. Table 1 shows the effect of the inlet gas concentration (C_{in}) on the removal efficiency. Results similar to SF_6 removal for several other gas pollutants are summarized in this table.

The effect of space velocity, SV , on the removal efficiency of SF_6 in N_2 is given in Figure 4. The inlet concentration, C_{in} , are 300 and 1.05 ppm at $I = 1.2 \text{ mA}$.

It is found that ψ decreases as SV increases. This is because, as SV increases, the mean residence time of the gas in the reactor decreases, thus lowering the chances of successful collisions between the electrons and gas molecules. Table 2 summarizes the effect of space velocity on the removal efficiency of several types of gases. The trend is the same as that of SF_6 . As can be seen in both Figures 3 and 4, the ψ measured from the experiments shows good agreement with the correlated ones, which are calculated using the model proposed by Tamon et al.¹⁷

Figure 5 shows CS_2 removal from N_2 with O_2 concentration ranging between 0–49.3%. In this figure, ψ^s defined by Eq. (2) is applied. It is obvious that ψ^s is greatly improved by the presence of oxygen. Also there exists an optimum O_2 concentration for maximum ψ^s . The effect of coexisting oxygen on the removal efficiency of certain gas samples is shown in Table 3. As seen in the table, most gaseous components show higher ψ^s as the percentage of O_2 becomes higher, except for the case of $C_2Cl_3F_3$ removal. In the case of $C_2Cl_3F_3$, it is surmised that electrons are consumed by reacting with the coexisting O_2 , so $C_2Cl_3F_3$ has less chances to react with electrons in N_2 - O_2 mixture than in N_2 . Another possible explanation for the decrease of ψ^s in the presence of O_2 in that radical reactions or the formation of the organic particles could be inhibited by the coexisting O_2 .

The removal results for COS in the presence of water vapor are shown in Figure 6. Evidently, the removal efficiency, ψ^s , is enhanced by the presence of H_2O . The formation of negative-ion clusters in the presence of H_2O could contribute to the higher removal efficiency. The experimental results for other gases are summarized in Table 4. Generally ψ^s increases with H_2O concentration.

The simultaneous effect of O_2 and H_2O on the removal efficiency is shown in Figure 7 and Table 5. Figure 7 shows the removal efficiency of SO_2 with 5.1% O_2 and 600–6,300 ppm H_2O . Also shown for comparison is the removal efficiency without O_2 but with 400 ppm H_2O . This result shows very high ψ^s in the high I range in the presence of O_2 . In the low I range, sufficient presence of H_2O raises ψ^s . However, the effect of H_2O on ψ^s is negligible in the high I range. On the contrary, the removal of CS_2 shows an opposite tendency, though the effect of H_2O is negligible in the high I range. This may be because of the formation of the by-product, COS.

SUMMARY OF PART I

Electron attachment reaction has been shown to be a promising treatment method for hazardous and malodorous gases such as SO_2 , H_2S , CH_3CHO , CH_3SH and $(\text{CH}_3)_2\text{S}$. Although most of the data in Tables 1~5 indicate imperfect removal efficiency, it can be expected that their removal efficiencies would be enhanced either by increasing the discharge current above that investigated in the present work or by adding another reactor in series. Another way to enhance the removal efficiency is to decrease the space velocity by reducing the gas flow rate or increasing the reactor length. It is also found that the lower the inlet gas concentration, the higher the removal efficiency becomes.

Furthermore, the experimental results reveal that the presence of some common coexisting gaseous components such as O_2 and H_2O in a gas mixture may positively or negatively affect the removal efficiency of the targeted gaseous pollutant.

PART II. EFFECT OF REACTOR STRUCTURE ON REMOVAL EFFICIENCY

As previously described in **Part I**, the electron attachment method has shown great promise for treatment of crematory emission and several gas pollutants. So far all experimental studies have been carried out using small electron attachment reactors. For on-site application, however the device needs to be scaled up 100 to 1000 times. To obtain a scale-up guideline, the effect of reactor structure on the removal efficiency must be understood. This is because any structural change is expected to affect simultaneously several important factors such as the discharge current, electron energy, electric field strength, migratory distance, and residence time in the reactor.

MATERIALS AND METHODS

The experimental apparatus used in this part is schematically identical to that shown in Figure 2, except for the structure of the reactor. Three effects of the reactor structure, namely, the cathode diameter, the anode shape, and the number of cathodes in the reactor on the removal efficiency with respect to CH_3I , CH_3CHO and $\text{C}_2\text{Cl}_3\text{F}_3$ have been investigated experimentally. In this part, the removal efficiency, ψ , defined by Eq. (1) is used in all experiments.

1. Influence of the cathode diameter

The experiments can be categorized into two parts: 1) removal from dry air (20% O_2), and 2) removal from dry N_2 . A variety of cathode diameters, 0.05, 0.1, 0.2, 0.3, 0.5, 0.8, 1.0, 1.26, and 1.6 mm, was tested. The diameter and length of the anode were 38 mm and 280 mm, respectively.

2. Influence of the anode shape

Three different shapes for the equivolume cylindrical reactor vessel, whose diameter (mm) and length (mm) are 76 x 70, (largest diameter), 38 x 280 (intermediate diameter), and 19 x 1,120 mm (smallest diameter), were tested. The cathode diameters used for the individual removal of CH_3I , $\text{C}_2\text{Cl}_3\text{F}_3$, and CH_3CHO were 0.3, 0.3, and 0.2 mm, respectively.

3. Influence of the number of cathodes

The cross section of the two reactor types are illustrated in Figure 8. Both have the same design features except for the number of cathode wires, one vs. five.

The diameter and length of the anode were 38 mm and 280 mm, respectively. The cathode diameter used for each gas was 0.3 mm.

RESULTS AND DISCUSSION

1. Influence of the cathode diameter

As mentioned earlier, the probability of electron attachment depends on electron energy and gas component. Electron energy in the reactor depends on the ratio of the electric field strength, E , to the total gas pressure, p , i.e. E/p . Electrons are accelerated in E , and collisions between electrons and gas molecules cause deceleration in p . Thus, if E/p is high, electron energy is also high. The electric field strength E is a function of r , as follows.

$$E = V/[r \ln (R/R_0)] \quad (3)$$

As seen in Eq. (3), electron energy increases when the corona voltage increases. Figure 9 shows the relation between the discharge current, I , and voltage, V , for CH_3I removal from air. Obviously, a thicker cathode diameter requires a significantly higher V to yield the same current. Similar tendency to the case of CH_3I removal from air also happens to CH_3I removal from N_2 as well as $\text{C}_2\text{Cl}_3\text{F}_3$ and CH_3CHO removal. According to Eq. (3), an increase in the cathode diameter, R_0 , contributes to an increase in E under a constant V . It can be said that the thicker the cathode diameter, the higher the electric field strength, E .

The average electric field strength per total pressure is given as follows.

$$\langle E/p \rangle = \frac{\int_{R_0}^R (2\pi r)(E/p)dr}{\pi (R^2/R_0^2)} = \frac{2V}{p(R+R_0) \ln (R/R_0)} \quad (4)$$

Figure 10 shows the observed $\langle E/p \rangle$ for CH_3I removal from air as a function of I . At the same discharge current I , the average value of $\langle E/p \rangle$ increases as the cathode diameter increases because a higher voltage V is required (see Figure 9). Thus the electron energy in Figure 10 increases with increasing cathode diameter.

Figure 11 shows the observed removal efficiency, ψ , for CH_3I removal from air corresponding to the different sizes of the cathode. It is found that a thicker

cathode provides a higher ψ . From Figures 10 and 11, it may be concluded that a high removal efficiency is attributable to a higher electron energy.

Although a thicker cathode wire provides a higher ψ , the required voltage, V , becomes higher as well, resulting in a higher power consumption. Figure 12 depicts ψ for CH_3I removal from air as a function of electric power, P . It conclusively shows that a thicker cathode provides a higher ψ when comparison is made at the same P . Figure 13 shows the effect of the cathode diameter on the removal of CH_3I from N_2 . The same conclusion on the cathode diameter is reached, as in the case of CH_3I removal from air (Figure 12). As another example, Figure 14 compares the removal efficiency of CH_3CHO from air vs. N_2 . Comparison of Figures 12 and 13, as well as Figure 14, reveals that a higher ψ is achieved for CH_3I and CH_3CHO in the presence of O_2 . Since O_3 can be generated from O_2 in the corona-discharge reactor, the significant enhancement in ψ may be ascribed to ozone oxidation.

2. Influence of the anode shape

Figure 15 compares the removal efficiency of $\text{C}_2\text{Cl}_3\text{F}_3$ from air among three anode (reactor) shapes. The order of efficiency is: smallest reactor diameter > intermediate diameter > largest diameter. Figure 16 shows the relations between ψ and P . It conclusively shows that the smaller the anode diameter, the higher the removal efficiency. Similar tendency was observed for the other cases.

The applied voltage and average E/p for $\text{C}_2\text{Cl}_3\text{F}_3$ removal from air are shown, respectively, in Figures 17 and 18. As seen in Figure 17, the larger the reactor diameter, the higher the required V . However, Figure 18 shows a different order of V vs. I from that of E/p vs. I in Figure 17. According to the typical electric field profile, this comparison suggests that the average electron energy in the smallest reactor diameter is largest, while the other two shapes have approximately the same electron energy.

From the previous discussion, it is found that ψ is enhanced as electron energy becomes higher. Since the orders of ψ vs. I and $\langle E/P \rangle$ vs. I differ as the anode shape changes, the difference in removal efficiency can not be attributed solely to the electron energy. The fact is that gas flow pattern inside the reactor is very complex. In a corona discharge, the ionized gas induces a gas convection, the so-called

"ion wind" or "corona wind". Since the wind velocity has been reported to be 1.5~2.0 m/s²², it can considerably flatten the overall gas velocity profile in the reactor, even if the superficial Reynolds number apparently indicates a conventional laminar flow regime. In other words, the reactor may be regarded as the plug-flow reactor (PFR).

In the case of a relatively short reactor, the reactor is closer to the completely stirred tank reactor (CSTR) more than PFR. Since the reaction rate here decreases as conversion increases, the PFR gives a higher conversion than CSTR. This explains why the 76 mm-diameter reactor has a significantly lower ψ than the 38 mm-diameter reactor even though their average $\langle E/p \rangle$ values are more or less equal.

One important conclusion is that to enhance the removal efficiency, the reactor should be as long and slender as technically feasible, provided the resulting higher velocity does not cause excessive pressure drop and turbulence. Efficiency enhancement could be obtained even when P , i.e. power consumption, is lowered significantly to achieve comparable average electron energy.

3. Influence of the number of cathodes

Figures 19 and 20 compare the effect of the cathode number on ψ for removal of CH_3CHO from air with respect to I and P , respectively. Using either criterion, the single-cathode reactor clearly exhibits higher efficiency than the 5-cathode one.

It was visually confirmed that, when high voltage was applied to the 5-cathode reactor, the corona of the central cathode failed to appear. This means that some "dead space" (corona-free space) existed around the central cathode wire. If there exists an electron-free space in the reactor, a part of the gas that passes through that electron-free space has no chance to collide with any electrons. In addition, the spatial distribution of electrons is not uniform in the 5-cathode reactor because the current is mainly generated in the region where each cathode is closest to the anode surface. In short, not only an electron-free space is found in the central region along the reactor axis but the electron-rich space occupies only some restricted space between the four cathodes and the outer anode. Therefore, the effective space inside the 5-cathode reactor is very small, thus leading to the low removal efficiency.

SUMMARY OF PART II

The structural effects of the corona-discharge reactor on gaseous removal of CH_3I , $\text{C}_2\text{Cl}_3\text{F}_3$ and CH_3CHO have been investigated. The experimental results reveal that the thicker the cathode, the higher the removal efficiency, provided the discharge voltage remains stable. Regarding the anode shape of equivolume reactors, it has been found that the smaller the reactor diameter, the higher the removal efficiency despite a lower energy consumption. As for the number of cathodes, the single-cathode reactor definitely exhibits higher removal efficiency than the 5-cathode one.

CONCLUSIONS AND RECOMMENDATIONS

Basic investigations on the important effects, namely, discharge current, inlet gas concentration, space velocity, and coexisting oxygen and water vapor on the individual removal efficiency of various kinds of gaseous pollutants have been carried out experimentally. It can be said that the electron attachment method shows good promise for treating several of the gaseous pollutants found in crematory emission.

According to the experimental results, a higher space velocity or inlet gas concentration causes a lower removal efficiency. On the other hand, a higher discharge current leads to a higher removal efficiency. The presence of either O_2 or H_2O in a gas mixture also plays an important role in the enhancement or, conversely, retardation of removal efficiency.

In addition, the effect of structural changes of the corona-discharge reactor on the gaseous removal efficiency has been investigated experimentally. The experimental data of this study would be very useful as guideline for scaling up the device. In conclusion, the most suitable structure of the corona-discharge reactor is the structure whose reactor diameter is the smallest and its single cathode wire is sufficiently thick. It is, however, necessary to carry out further study on the simultaneous removal of several coexisting gaseous components which are found in crematory emission.

ACKNOWLEDGEMENT

The present work is a part of a bilateral Research Collaboration Project whose Thai side is supported by a two-year grant from the National Research Council of Thailand. Mr. Kittisak Larpsuriyakul spent one year (1995-1996) in Prof. Okazaki's Lab under an Exchange Program sponsored by the Association of International Education Japan. Dr. Wiwut Tanthapanichakoon receives financial support from Thailand Research Fund (1996-1999) and he also made a short-term visit in 1994 under JSPS Exchange Scheme. The support rendered by NRCT, TRF, AIEJ and JSPS are gratefully acknowledge. On the Japanese side financial support was supplied by the Ministry of Education, Scienc, Sports and Culture of Japan through a Grant-in-Aid on Development of Scientific Research No. 0555211 (1994).

NOMEMCLATURE

C	=	concentration [ppm]
E	=	electric field [Vm^{-1}]
I	=	discharge current [mA]
P	=	power consumption [W]
P	=	pressure [Pa]
R	=	radius of the reactor anode [m]
R_0	=	radius of the reactor cathode [m]
r	=	coordinate along the radius [m]
SV	=	space velocity [h^{-1}]
V	=	discharge voltage [V]

<Subscript>

in	=	inlet of reactor
out	=	outlet of reactor

REFERENCES

1. Caledonia, G.E. A Survey of the Gas-Phase Negative Ion Kinetics of Inorganic Molecules. Electron Attachment Reactions. *Chem. Rev.*, 1975, **75**, 333-351.
2. Larpsuriyakul, K., Sano, N., Tamon, H., Tanthapanichakoon, W. and Okazaki, M. Influence of Structure of Corona-Discharge Reactor on Removal of Dilute Gases Using Electron Attachment. *Proc. Himeji Conf. Soc. Chem. Engrs. Japan*, 1996, 270-271.
3. Larpsuriyakul, K., Charinpanitkul, T., Tanthapanichakoon, W., Sano, N., Tamon, H. and Okazaki, M. Removal of Dilute Gaseous Impurities by Electron Attachment Reaction Using Corona-Discharge Reactors of Different Structures. *7th National Conf. Chem. Eng. and Appl. Chemistry, Chiang Mai*, 24-25 October 1997.
4. Löffler, F. Staubabscheiden. Thieme Verlag, Stuttgart, 1988.
5. Massey, S. H. Negative Ions. Cambridge University Press, Cambridge, 1976.
6. Massey, S.H. Atomic and Molecular Collisions. Taylor & Francis, London, 1979.
7. Nishida, K. and Matsuda Y. Molodor of Exhaust Gas from Crematory. *J. Odor Control*, 1981, **10**, 1-11. (in Japanese)
8. Nishida, K. Malodor at Cremation Facility (Part I). *PPM*, 1988, **3**, 49-58. (in Japanese)
9. Nishida, K. Malodor at Cremation Facility (Part II). *PPM*, 1988, **4**, 51-59. (in Japanese)
10. Ogawa A. Separation of Particles from Air and Gases, Vol. II. CRC Press, Florida, 1984.
11. Oglesby, S. and Nichols, G.B. Electrostatic Precipitation. Marcel Dekker, New York, 1978.
12. Sano, N., Nagamoto, T., Tamon, H. and Okazaki, M. Removal of Iodine and Methyl Iodide in Gas by Wetted-Wall Reactor Based on Selective Electron Attachment. *J. Chem. Eng. Japan*, 1996, **29**, 59-64.
13. Sano, N. Development of Gas Purification Technology by Selective Electron Attachment. *Doctor Thesis, Kyoto University, Kyoto*, 1997.
14. Sano, N., Nagamoto, T., Tamon, H., Suzuki, T. and Okazaki, M. Removal of Methyl Iodide in Gas by Corona-Discharge Reactor. *J. Chem. Eng. Japan*, 1997a. (in press)
15. Sano, N., Nagamoto, T., Tamon, H., Suzuki, T. and Okazaki, M. Removal of Acetaldehyde and Skatole in Gas by Corona-Discharge. *Ind. Eng. Chem. Res.*, 1997b, **36**, 3783-3791.
16. Tamon, H., Yano, H. and Okazaki, M. A New Method of Gas Mixture Separation Based on Selective Electron Attachment. *Kagaku Kogaku Ronbunshu*, 1989, **15**, 663-668.
17. Tamon H., Mizota, H., Sano, N., Schulze, S. and Okazaki, M. New Concept of Gas Purification by Electron Attachment. *AIChE J.*, 1995, **41**, 1701-1711.
18. Tamon, H., Sano, N. and Okazaki, M. Influence of Oxygen and Water Vapor on Removal of Sulfur Compounds by Electron Attachment. *AIChE J.*, 1996, **42**, 1481-1486.

19. Tanthapanichakoon, W., Larpsuriyakul, K., Sano, N., Tamon, H. and Okazaki, M. Effect of Reactor Structure on Removal of Methyl Iodide and Chlorofluorocarbon in Gas Using Selective Electron Attachment. *Proc. Regional Sym. Chem. Eng., Jakarta*, October 1996, 3.2.1-3.2.14.
20. Tanthapanichakoon, W., Larpsuriyakul, K., Charinpanitkul, T., Sano, N., Tamon, H. and Okazaki, M. Effect of Structure of Corona-Discharge Reactor on Removal of Dilute Gaseous Pollutants Using Selective Electron Attachment. *J. Chem. Eng. Japan*, 1998, **31**. (in press)
21. White, H. L. Industrial Electrostatic Precipitation. Addison-Wesley, London, 1963.
22. Yabe, A., Mori, Y. and Hijikata, K. EHD Study of the Corona Wind between Wire and Plate Electrode. *AIAA J.*, 1978, **16**, 340.

Table 1. Effect of inlet gas concentration on removal efficiency

Sample gas	Experimental conditions					Removal efficiency		
	I [mA]	SV [h ⁻¹]	C_{in} [ppm]	C_{O_2} [%]	C_{H_2O} [ppm]	Change of ψ		ψ^*_{max} [-]
						I	C_{in}	
SF ₆	0.25~1.6	18.9	0.176~298	0	0	incr.	decr.	1.0
SO ₂	0.25~1.6	18.9	32.7~304	0	0	incr.	decr.	0.44
(CH ₃) ₂ S	0.25~1.5	18.9	3.88~89	0	0	incr.	decr.	0.90
CH ₃ I	0.1~2.0	47.3	27.6~144.3	0	0	incr.	decr.	0.65
C ₂ Cl ₃ F ₃	0.1~3.0	18.9	50~400	0	0	incr.	decr.	1.0
CH ₃ CHO	0.1~1.0	21.8	9.9~35.6	0	0	incr.	decr.	0.88
(CH ₃) ₃ N	0.5~1.0	58.6	43	0	0	incr.	-	0.40

* Maximum ψ observed among all experiments

Table 2. Effect of space velocity on removal efficiency

Sample gas	Experimental conditions					Removal efficiency		
	I [mA]	SV [h ⁻¹]	C_{in} [ppm]	C_{O_2} [%]	C_{H_2O} [ppm]	Change of ψ		ψ^*_{max} [-]
						I	C_{in}	
SF ₆	1.2	4.7~163	1.05	0	0	-	decr.	1.0
CH ₃ I	0.1~2.0	24.6~76.1	81.5	0	0	incr.	decr.	0.80
CH ₃ CHO	0.25~1.5	21.8~66.2	35.6	0	0	incr.	decr.	0.70

* Maximum ψ observed among all experiments

Table 3. Effect of coexisting oxygen on reaction by-products and removal efficiency

Sample gas	Experimental conditions					Reaction by-product	Removal efficiency		
	I	SV	C_{in}	C_{O_2}	C_{H_2O}		Change of ψ^s		ψ^s_{max} [-]
	[mA]	[h ⁻¹]	[ppm]	[%]	[ppm]		I	C_{in}	
SO ₂	0.25~1.5 (10.1~4.5)	18.9	101	0~18	0	none	incr.*	incr.*	0.95
CS ₂	0.18~1.5 (9.3~14.8)	18.9	30	0~49	0	SO ₂ COS	incr.	max. at 2%*	0.98
COS	0.2~1.5 (9.5~14.8)	18.9	29	0~50	0	SO ₂	incr.	max. at 2%	0.92
CH ₃ SH	0.05~1.0 (6.3~14.9)	18.9	69	0~20	0	SO ₂ H ₂ S or COS	incr.	incr.	1.0
(CH ₃) ₂ S	0.25~1.0 (6.0~10)	18.9	70	0~22	0	none	incr.	incr.	1.0
C ₂ Cl ₃ F ₃	0.1~1.5 (9.2~15.2)	18.9	400	0~20	0	HCl or HF	incr.	decr.	0.88**
(CH ₃) ₃ N	0.05~0.15 (8.3~14.0)	69.4	25	0~20	0	CH ₃ CHO, C ₂ H ₅ OH, (CH ₃) ₂ CO or CH ₃ NO ₂	incr.	incr.	1.0**

* ψ^s for SO₂ increases with discharge current; ψ^s of SO₂ increases with the concentration of O₂; ψ^s of CS₂ becomes maximum at 2% of O₂ concentration.

** Maximum ψ is calculated by Eq. (1).

Table 4. Effect of coexisting water vapor on reaction by-products and removal efficiency

Sample gas	Experimental conditions					Reaction by-product	Removal efficiency		
	I	SV	C_{in}	C_{O_2}	C_{H_2O}		Change of ψ^s		ψ^s_{max}
	[mA]	[h ⁻¹]	[ppm]	[%]	[ppm]		I	C_{H_2O}	
H ₂ S	0.2~1.45 (3.5~8.7)	37.8	60	0	400~11,000	none	incr.	incr.	1.0
SO ₂	0.25~1.5 (4.5~5.7)	37.8	122	0	400~13,000	none	incr.	incr.	0.39
CS ₂	0.25~1.4 (4.9~7.5)	37.8	48	0	300~11,000	SO ₂ COS	incr.	incr.	0.66
COS	0.25~1.5 (4.5~5.7)	37.8	53	0	650~10,000	SO ₂	incr.	incr.	0.64
CH ₃ SH	0.1~1.5 (4.8~6.5)	37.8	40	0	1,000~10,000	SO ₂	max. at 0.25~0.5 mA	incr.	0.65
(CH ₃) ₂ S	0.25~1.5 (4.5~5.6)	52.9	38	0	1,100~9,100	SO ₂	max. at 0.5 mA	incr.	0.27

Table 5. Effect of coexisting water vapor on reaction by-products and removal efficiency in presence of oxygen

Sample gas	Experimental conditions					Reaction by-product	Removal efficiency		
	I	SV	C_{in}	C_{O_2}	C_{H_2O}		Change of ψ^s		ψ^s_{max}
	[mA]	[h ⁻¹]	[ppm]	[%]	[ppm]		I	C_{H_2O}	
SO ₂	0.25~1.5 (9.0~14.5)	37.8	120	5.0	600~6,300	none	incr.	incr.*	0.89
CS ₂	0.25~1.5 (8.5~14.0)	37.8	65	14.5	600~9,500	SO ₂ COS	incr.	decr.	0.93
(CH ₃) ₂ S	0.1~1.5 (8.0~14.0)	52.9	39	7.9	600~5,600	SO ₂	incr.	incr.	0.98

* Negligible in high discharge current

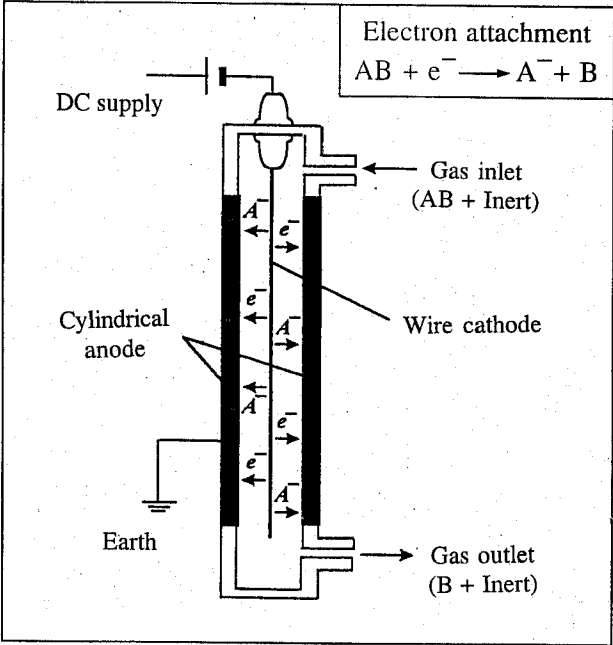


Fig 1. Principle of gas purification

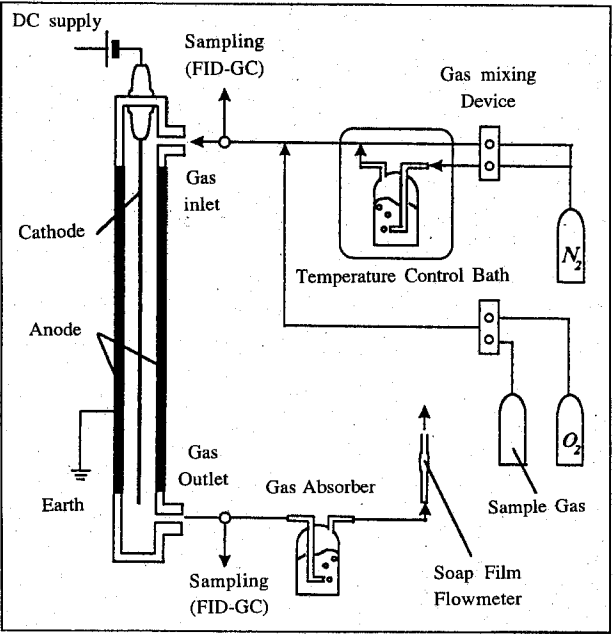


Fig 2. Schematic diagram of experimental apparatus

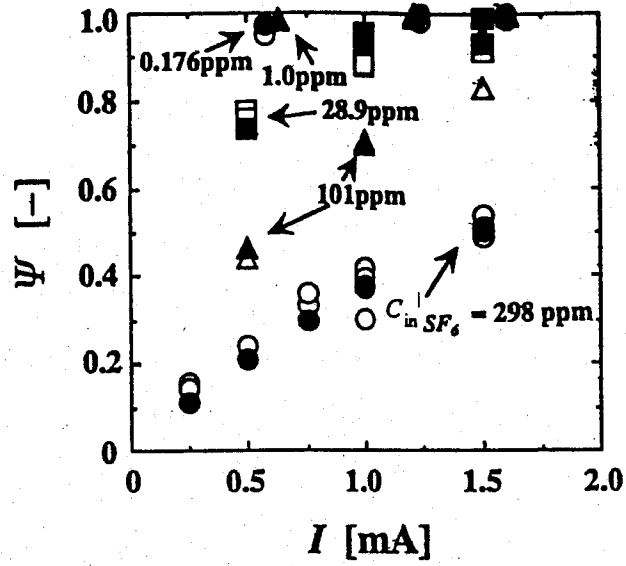


Fig 3. Removal efficiency of SF_6 from N_2 : $\text{SV} = 18.9 \text{ h}^{-1}$;
(open symbol, measured; filled symbol, correlated)

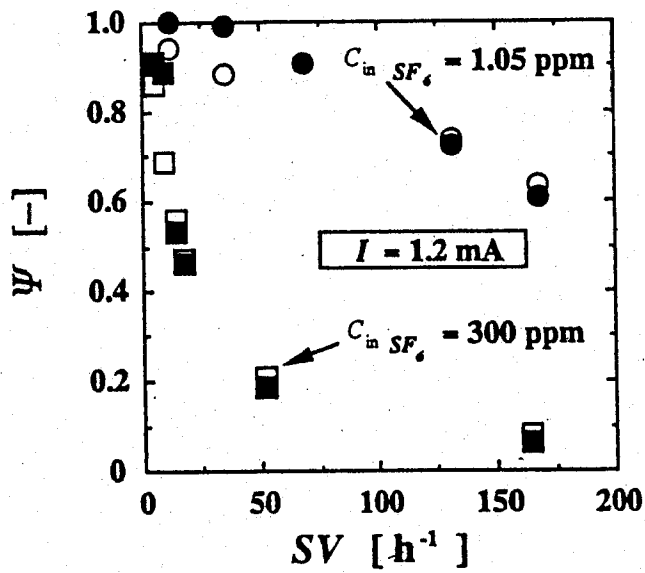


Fig 4. Influence of gas flow rate on removal efficiency of SF_6 ;
(open symbol, measured; filled symbol, correlated)

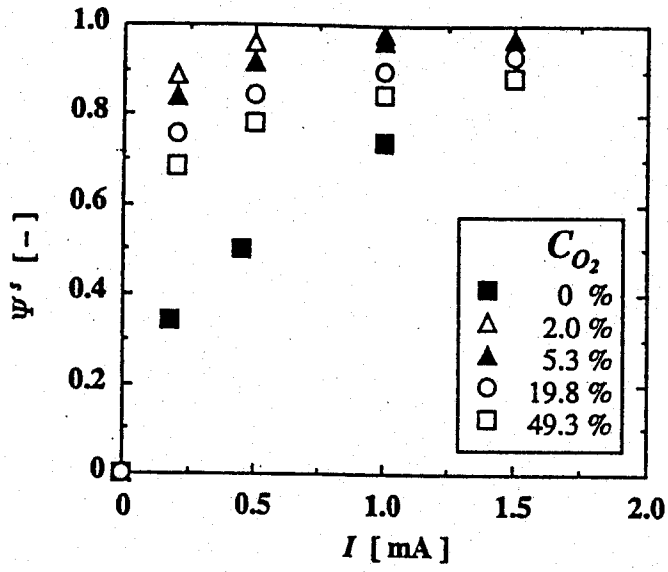


Fig 5. Removal efficiency of CS_2 in presence of O_2 :
 $C_{in} = 29.8$ ppm, $SV = 18.9$ h⁻¹

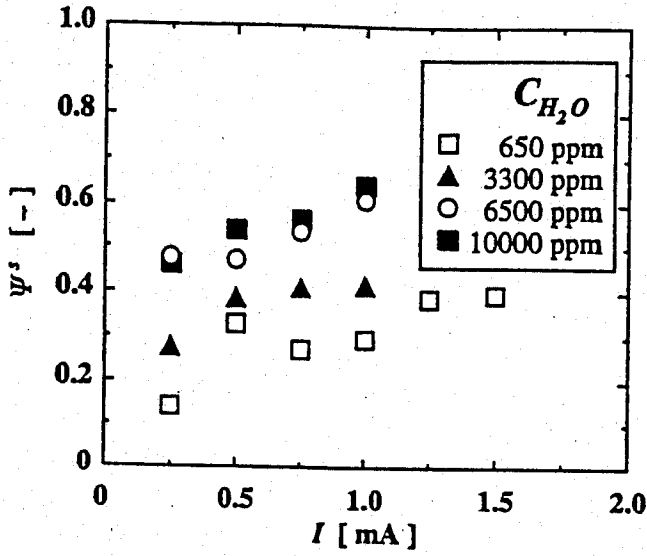


Fig 6. Removal efficiency of COS in presence of H_2O :
 $C_{in} = 52.8$ ppm, $SV = 37.8$ h⁻¹

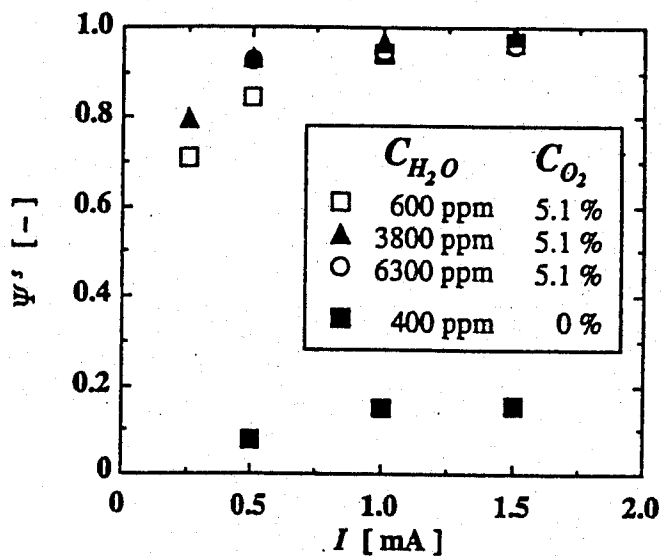


Fig 7. Removal efficiency of SO_2 in presence of O_2 and H_2O :
 $C_{in} = 120.0$ ppm, $SV = 37.8$ h⁻¹

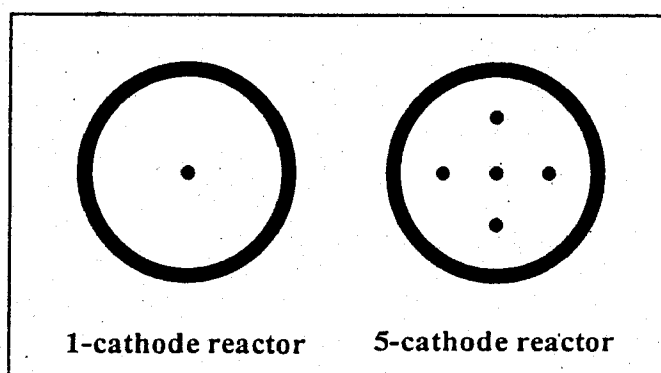


Fig 8. Cross sections of two types of reactor

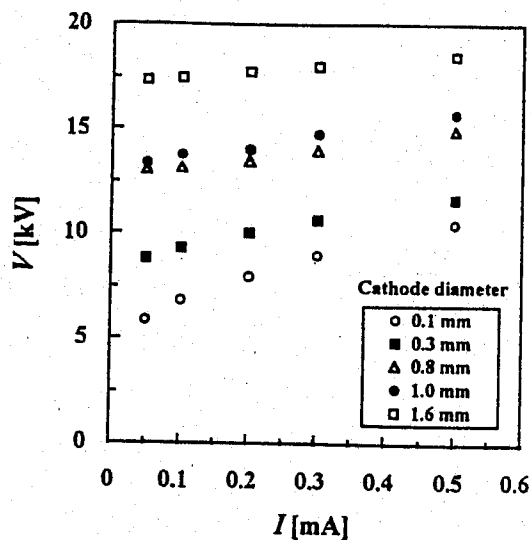


Fig 9. Discharge current-voltage relationship for CH_3I removal from air (20% O_2); (anode diameter x length = 38 mm x 280 mm, $C_{\text{in}} = 80$ ppm, $SV = 46.3 \text{ h}^{-1}$)

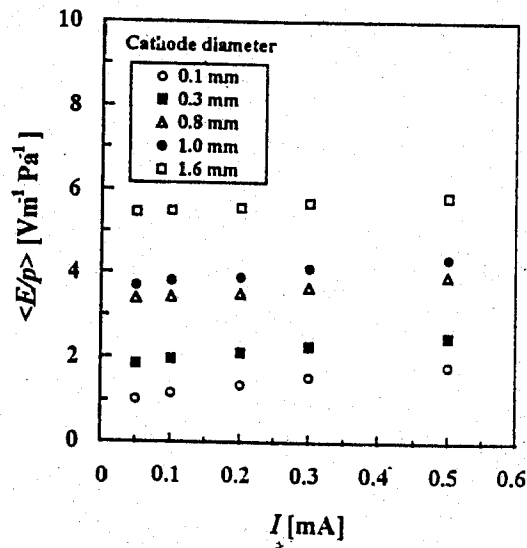


Fig 10. Average electric field strength/pressure as a function of discharge current for CH_3I removal from air (20% O_2); (anode diameter x length = 38 mm x 280 mm, $C_{\text{in}} = 80$ ppm, $SV = 46.3 \text{ h}^{-1}$)

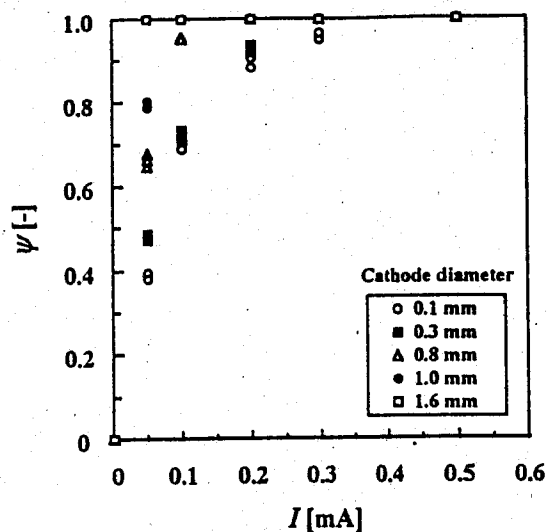


Fig 11. Removal efficiency of CH_3I from air (20% O_2) as a function of discharge current; (anode diameter x length = 38 mm x 280 mm, $C_{\text{in}} = 80$ ppm, $\text{SV} = 46.3 \text{ h}^{-1}$)

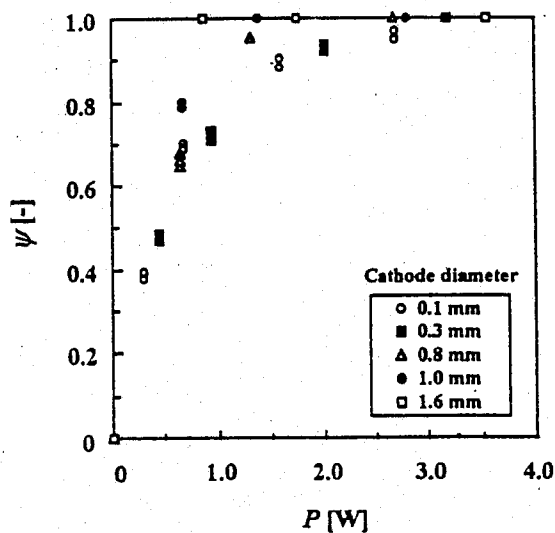


Fig 12. Removal efficiency of CH_3I from air (20% O_2) as a function of electric power; (anode diameter x length = 38 mm x 280 mm, $C_{\text{in}} = 80$ ppm, $\text{SV} = 46.3 \text{ h}^{-1}$)

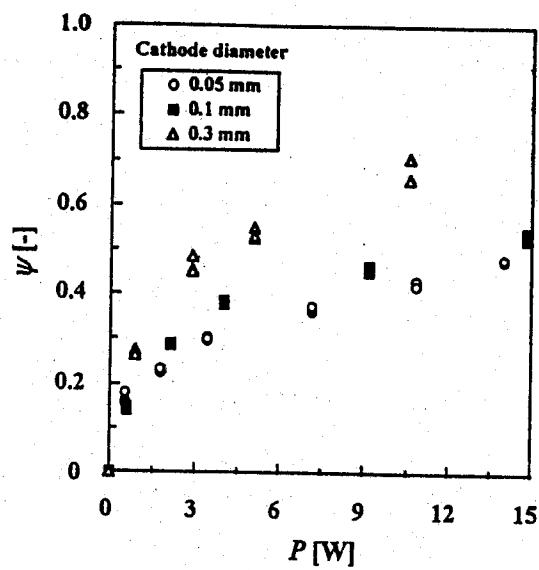


Fig 13. Removal efficiency of CH_3I from N_2 as a function of electric power; (anode diameter x length = 38 mm x 280 mm, cathode diameter = 0.3 mm, C_{in} = 100 ppm, SV = 56.7 h^{-1})

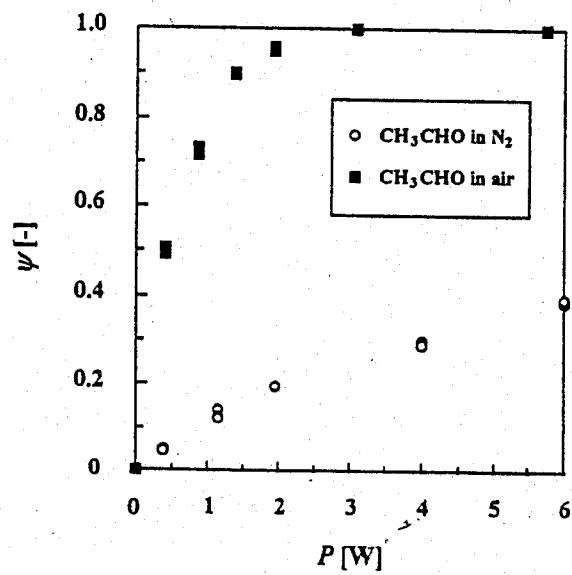


Fig 14. Comparison of removal efficiencies of CH_3CHO removal from air vs. N_2 ; (anode diameter x length = 38 mm x 280 mm, C_{in} = 100 ppm, SV = 56.7 h^{-1})

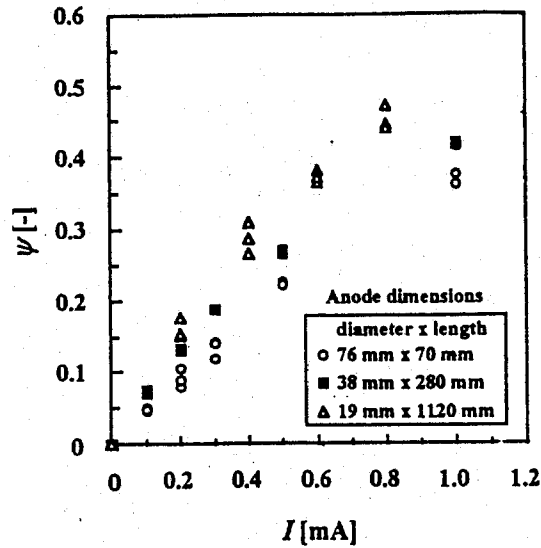


Fig 15. Removal efficiency of $C_2Cl_3F_3$ from air (20% O_2) as a function of discharge current; (cathode diameter = 0.3 mm, C_{in} = 400 ppm, SV = 18.9 h^{-1})

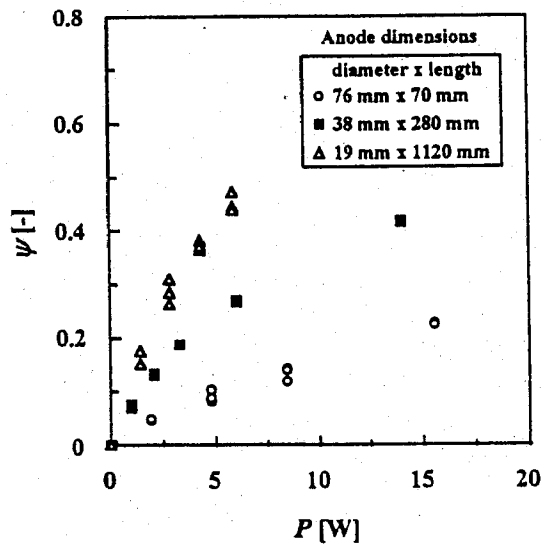


Fig 16. Removal efficiency of $C_2Cl_3F_3$ from air (20% O_2) as a function of electric power; (cathode diameter = 0.3 mm, C_{in} = 400 ppm, SV = 18.9 h^{-1})

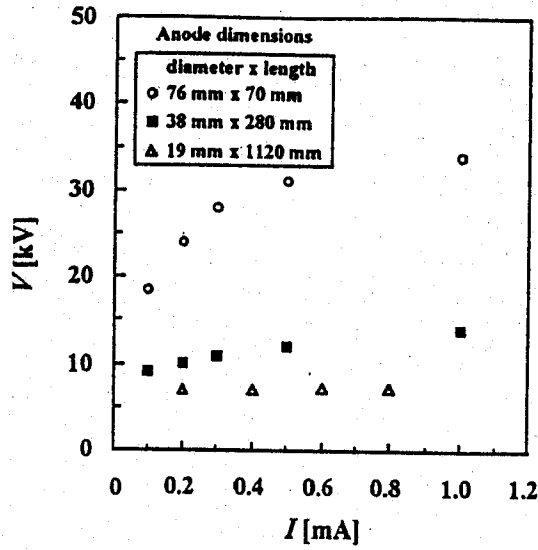


Fig 17. Discharge current-voltage relationship for $C_2Cl_3F_3$ removal from air (20% O_2); (cathode diameter = 0.3 mm, C_{in} = 400 ppm, SV = 18.9 h^{-1})

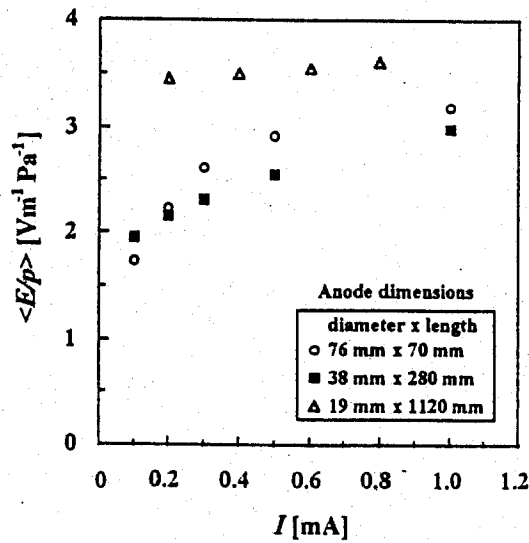


Fig 18. Average electric field strength/pressure as a function of discharge current for $C_2Cl_3F_3$ removal from air (20% O_2); (cathode diameter = 0.3 mm, C_{in} = 400 ppm, SV = 18.9 h^{-1})

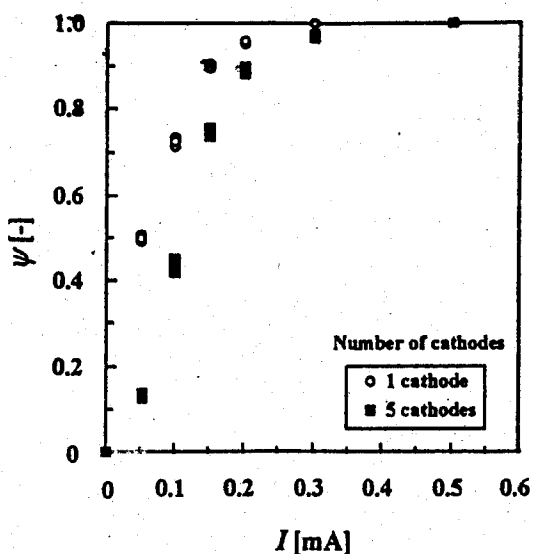


Fig 19. Removal efficiency of CH_3CHO from air (20% O_2) as a function of discharge current; (cathode diameter = 0.3 mm, anode diameter x length = 38 mm x 280 mm, C_{in} = 100 ppm, SV = 56.7 h^{-1})

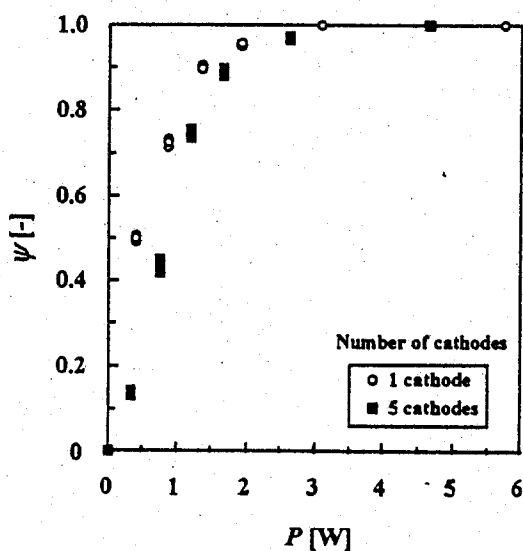


Fig 20. Removal efficiency of CH_3CHO from air (20% O_2) as a function of electric power; (cathode diameter = 0.3 mm, anode diameter x length = 38 mm x 280 mm, C_{in} = 100 ppm, SV = 56.7 h^{-1})